AIP Applied Physics Letters

Enforced c-axis growth of ZnO epitaxial chemical vapor deposition films on a-plane sapphire

Yong Xie, Manfred Madel, Thilo Zoberbier, Anton Reiser, Wanqi Jie et al.

Citation: Appl. Phys. Lett. **100**, 182101 (2012); doi: 10.1063/1.4709430

View online: http://dx.doi.org/10.1063/1.4709430

View Table of Contents: http://apl.aip.org/resource/1/APPLAB/v100/i18

Published by the American Institute of Physics.

Related Articles

GaP heteroepitaxy on Si(001): Correlation of Si-surface structure, GaP growth conditions, and Si-III/V interface structure
J. Appl. Phys. 111, 083534 (2012)

Substrate-assisted nucleation of ultra-thin dielectric layers on graphene by atomic layer deposition
Appl. Phys. Lett. 100, 173113 (2012)

Role of plasma activation in kinetics of carbon nanotube growth in plasma-enhanced chemical vapor deposition
J. Appl. Phys. 111, 074307 (2012)

GaN based nanorods for solid state lighting
App. Phys. Rev. 2012, 5 (2012)

GaN based nanorods for solid state lighting
J. Appl. Phys. 111, 071101 (2012)

Additional information on Appl. Phys. Lett.

Journal Homepage: http://apl.aip.org/

Journal Information: http://apl.aip.org/about/about_the_journal

Top downloads: http://apl.aip.org/features/most_downloaded

Information for Authors: http://apl.aip.org/authors

ADVERTISEMENT

ACCELERATE AMBER AND NAMD BY 5X.
TRY IT ON A FREE, REMOTELY-HOSTED CLUSTER.
LEARN MORE

Enforced *c*-axis growth of ZnO epitaxial chemical vapor deposition films on *a*-plane sapphire

Yong Xie,[1,2,a)] Manfred Madel,[2] Thilo Zoberbier,[2,3] Anton Reiser,[2] Wanqi Jie,[1] Benjamin Neuschl,[2] Johannes Biskupek,[3] Ute Kaiser,[3] Martin Feneberg,[2,4] and Klaus Thonke[2,b)]

[1]*State Key Laboratory of Solidification Processing, School of Materials Science and Engineering, Northwestern Polytechnical University, 710072 Xi'an, China*
[2]*Institut für Quantenmaterie/Gruppe Halbleiterphysik, Universität Ulm, 89069 Ulm, Germany*
[3]*Materialwissenschaftliche Elektronenmikroskopie, Universität Ulm, 89069 Ulm, Germany*
[4]*Institut für Experimentelle Physik, Otto-von-Guericke-Universität Magdeburg, 39106 Magdeburg, Germany*

(Received 27 February 2012; accepted 15 April 2012; published online 30 April 2012)

To enforce perfect *c*-axis orientation of ZnO epitaxial films grown on *a*-plane sapphire, we first grew perfectly perpendicularly aligned (i.e., c axis oriented) ZnO nanopillars on such sapphire substrates, and then over-grew these by a closed epitaxial film using a modified chemical vapor deposition process at atmospheric pressure. X-ray diffraction and low temperature photoluminescence measurements confirm the desired epitaxial relationship and very high crystalline quality. This growth scheme is an efficient method to suppress dislocations and polycrystalline growth of ZnO and could work equally well for other heteroepitaxial epilayer/substrate systems. © *2012 American Institute of Physics*. [http://dx.doi.org/10.1063/1.4709430]

Due to its wide band gap of 3.37 eV at 300 K, the large exciton binding energy (60 meV), the piezo-electric properties, its bio-capability, etc., zinc oxide (ZnO) became a promising material in optoelectronics and other fields.[1,2] In recent years, different growth methods like metal organic chemical vapor deposition (MOCVD),[3,4] pulsed laser deposition (PLD),[5,6] molecular beam epitaxy (MBE),[7] etc. allowed to grow high quality ZnO films and quantum wells. There are fewer reports available about the simple and low cost chemical vapor deposition (CVD) process, and only few reports about using bulk ZnO single crystals or GaN as substrates.[8] Very recently, epitaxial ZnO CVD films were grown on $\gamma-\mathrm{LiAlO_2}(100)$.[9] However, although the structural quality of the layers grown on $\gamma-\mathrm{LiAlO_2}(100)$ is quite high, the high costs of the substrates and the limited optical quality in terms of photoluminescence (PL), which are still far inferior compared to those of films grown on GaN or bulk ZnO, are a major drawback.

Besides solving the p-type doping problem, the reduction of the dislocation density and suppression of stacking faults is a major challenge in the growth of ZnO films to obtain material suited for applications in optical devices like light-emitting diodes (LEDs) and laser diodes. There are basically two approaches possible to reduce the dislocation density: (i) choosing a substrate with less mismatch to the epilayer (e.g., ZnO single crystals) and (ii) using a special nucleation layer or inserting strain relaxing layers in a "multi-step growth."[6] *A*-plane sapphire is frequently chosen as a substrate to grow high quality *c*-axis oriented ZnO nanowires. The background is that the 4-fold of the ZnO "a" lattice constant fits perfectly to the "c" lattice constant of sapphire with a mismatch of less than 0.08% at room temperature (more precisely: $4\times \mathrm{a(ZnO)} = 4\times 3.249$ Å $= 12.996$ Å; $\mathrm{c(Al_2O_3)} = 12.99$ Å, where the axis alignment is $\hat{c}_{\mathrm{ZnO}} \parallel \hat{a}_{\mathrm{Al_2O_3}}, \hat{a}_{\mathrm{ZnO}} \parallel \hat{c}_{\mathrm{Al_2O_3}}$, and $\hat{\mathrm{m}}_{\mathrm{ZnO}} \parallel \hat{m}_{\mathrm{Al_2O_3}}$). This small mismatch governs the growth orientation of ZnO nanowires or ZnO epitaxial layers.[10,11] Besides this expected growth of the ZnO nanowires in c-direction, frequently also growth of ZnO films with an alternative orientation $[01\bar{1}1]_{\mathrm{ZnO}} \parallel [11\bar{2}0]_{\mathrm{Al_2O_3}}$ is reported.[17] In this paper, we report a method to enforce monocrystalline c-axis growth of ZnO films by overgrowth of *c*-oriented ZnO-nanopillars on *a*-plane sapphire substrates using a modified CVD process.

All growth experiments were performed in a horizontal three-zone oven equipped with a quartz glass liner tube. In a first step, ZnO nanopillars were grown on a ZnO seed layer using a carbon-thermal method as reported by our group previously.[12] Briefly, zinc acetate dihydrate heated up to 220 °C was used as a precursor, and the *a*-plane sapphire substrate was kept at a temperature of 500 °C under a pressure of 500 mbar. The growth process of the seed layer took 3 min. For the next growth step, the sample was placed without any further treatment into the same growth tube and heated now up to 850 °C. A 1:1 molar mixture of ZnO (purity 5N5, Alfa Aesar) and graphite powder (purity 6N, Alfa Aesar, 200 mesh) was heated up to 1060 °C for 30 min to obtain perfectly perpendicularly aligned ZnO nanopillars. Finally, ZnO powder (Grillo, P4, purity 99.99%) and isopropanol were used as precursors for the ZnO film growth. The reaction took place at a temperature of 950 °C for the ZnO powder mixture and a temperature of 800 °C for the substrate, respectively. The pressure was set to slightly below atmospheric pressure (845 mbar). A flow of 84 standard cubic centimeters per minute (sccm) argon was used as carrier gas, and a 3 sccm oxygen stream was added to react with the organic precursor. Details of the ZnO film growth process will be reported elsewhere.[13]

The sample morphology was characterized by field-emitter scanning electron microscopy (FE-SEM, LEO 982).

a)Electronic mail: xieyong.nwpu@gmail.com.
b)Electronic mail: klaus.thonke@uni-ulm.de.

 © 2012 American Institute of Physics

The epitaxial relationship between the ZnO film and the *a*-plane sapphire was examined using a Philips CM20 transmission electron microscope (TEM) operating at 200 keV. X-ray diffraction (XRD, Siemens D5000) was used to characterize the crystal quality and epitaxial orientation of the ZnO layer. PL spectra were recorded at liquid helium temperature, and a cw HeCd laser served as excitation source (10 mW, $\lambda = 325$ nm). The emitted light was collected by a monochromator equipped with a 1200 groves/mm grating and recorded by a liquid-nitrogen cooled UV-optimized CCD camera. The spectral resolution of the system was better than 100 μeV.

Figures 1(a) and 1(b) show SEM micrographs of the morphology of the as-grown ZnO nanopillars and of the final ZnO film, respectively. From the top view of the ZnO nanopillars, we can see that at least the upper part of all pillars is oriented perpendicular to the sapphire substrate. They all show six clear-cut facets, proving the c-axis to be the long axis and growth direction. The side facets (=*m* planes) of all of them show the same orientation, i.e., the same rotational orientation relative to the substrate. This way, the arrangement of any epitaxial layer to fill the gaps between the pillars later on is totally fixed. The resulting ZnO film (Fig. 1(b)) shows a rather smooth surface with a number of very shallow (<50 nm) hexagonal depressions, much less roughness (<5 nm) and defects than found for similar layers grown by CVD or other methods directly on a-plane sapphire substrates.[9]

To clarify the crystallographic relationship between the epitaxial ZnO layer and the substrate, we used XRD ($\omega - 2\theta$)- and ϕ-scans of both the ZnO layer and the sapphire substrate. Fig. 2(a)) shows the result of the ($\omega - 2\theta$)-scan of the ZnO film. The ZnO film has clearly a *c*-plane surface, which means $[0001]_{ZnO} \parallel [11\bar{2}0]_{Al_2O_3}$. However, two orders of magnitude lower in intensity, we also find a very weak peak for the $(01\bar{1}1)$ plane of ZnO, which is commonly observed for ZnO nanowires and films grown on *a*-plane sapphire, and means that minor mis-oriented inclusions must be present.[12,17] For the in-plane orientational relationship between the ZnO film and the sapphire substrate, ϕ scans of both the $(22\bar{4}6)$ plane of sapphire and the $(11\bar{2}4)$ plane of ZnO were measured (Fig. 2(b)). Six peaks showing the hexagonal symmetry were clearly verified for a full rotation of the ZnO film, which show no rotational domains or twinning of the film.[11]

Figure 3(a) shows a TEM weak-beam dark-field (WBDF) micrograph of a cross section of the ZnO layer on the sapphire substrate, which was acquired close to the $[10\bar{1}0]$ zone by exploiting the $g \cdot b$ criterion along the $1\bar{2}10$ reflection using the 3g-condition. The dislocation density decreases along the growth direction. The interfaces between the top of the original ZnO nanopillars and the final film in some places can be retrieved as very faint dislocation lines parallel to the surface (as marked, e.g., by the arrow in Fig. 3(a)). Typical selected area diffraction (SAED) patterns of the substrate alone (Fig. 3(b)) and of both the substrate

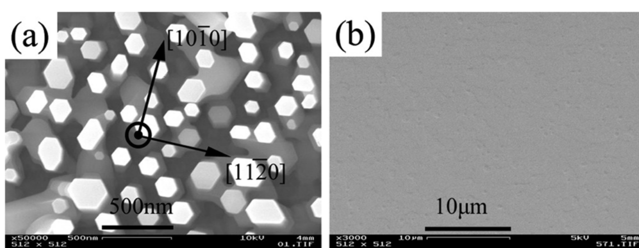

FIG. 1. (a) SEM top-view of as-grown ZnO nanopillars and (b) ZnO film grown on *a*-plane sapphire.

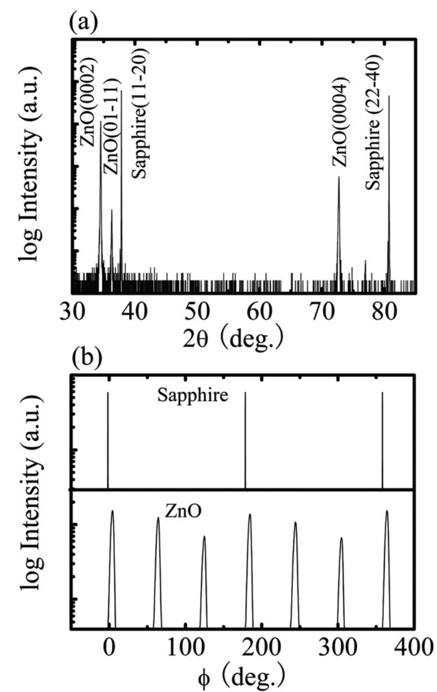

FIG. 2. (a) $\omega - 2\theta$ of a ZnO film grown on *a*-plane sapphire. (b) ϕ scan of the sapphire $(22\bar{4}6)$ plane and of the ZnO $(11\bar{2}4)$ plane.

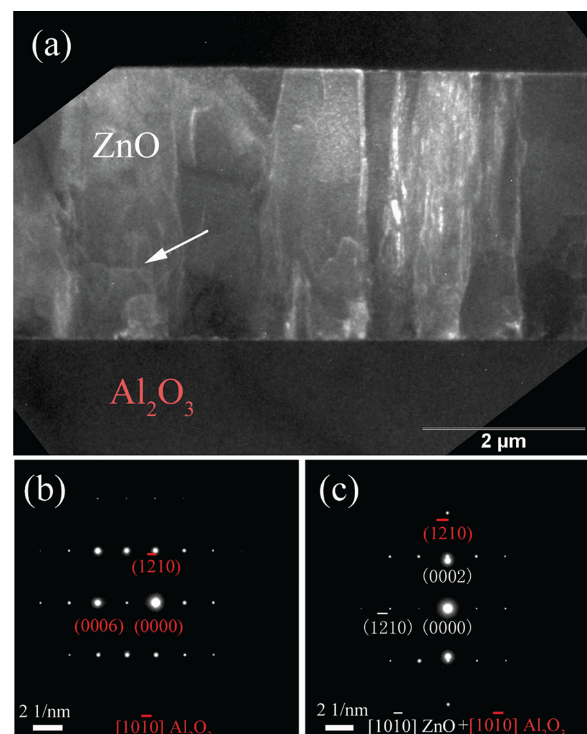

FIG. 3. (a) TEM weak-beam dark-field image of the ZnO film grown on *a*-plane sapphire. The arrow marks a dislocation. (b) and (c) SAED patterns acquired along the $[10\bar{1}0]$ zone axis of sapphire and ZnO, respectively.

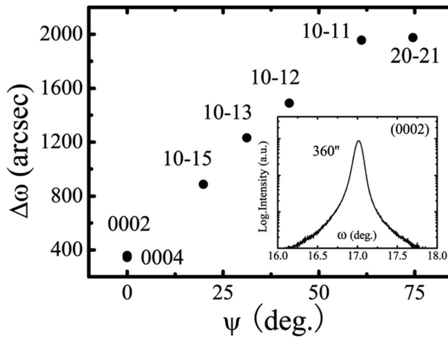

FIG. 4. The FWHMs of rocking curves of ZnO film grown on *a*-plane sapphire as a function of ψ. The inset shows the (0002) plane rocking curve.

plus layer (Fig. 3(c)) also show the crystallographic relationship. The $[10\bar{1}0]$ diffraction pattern of the ZnO film was clearly observed.

Besides the orientation, also the crystal quality was characterized by recording XRD rocking curves in skewed geometry. As shown in Fig. 4, the full width at half maximum (FWHM) of the reflexes is plotted against the angle ψ which corresponds to the tilt angle of the plane normal relative to $\langle 0001 \rangle$-direction. The (0002) reflex shows a FWHM of 360 arcsec (Fig. 4, inset), which is comparable to films grown by other methods like PLD (see, e.g., Ref. 14, where a FWHM of (0002) plane of 370 arcsec was quoted). As the FWHM of the (0002) and (0004) reflexes is nearly the same, the broadening of these reflexes must originate mostly from tilt and twist of the crystallites due to screw type and edge type dislocations. Any broadening due to limited lateral coherence length of the ZnO nano-crystallites in the film, which would result in smaller $\Delta\omega$ for the (0004) reflex than for the (0002) reflex, can be excluded. Thus, it is possible to estimate the dislocation densities from the FWHM of (0002) and $(20\bar{2}1)$ using the relations given by Dunn and Kogh,[15]

$$\rho_{\text{screw}} = \frac{\Delta\omega^2_{0002}}{4.35 \cdot |\mathbf{b}_{\text{screw}}|^2}, \quad \rho_{\text{edge}} = \frac{\Delta\omega^2_{20\bar{2}1}}{4.35 \cdot |\mathbf{b}_{\text{edge}}|^2}, \quad (1)$$

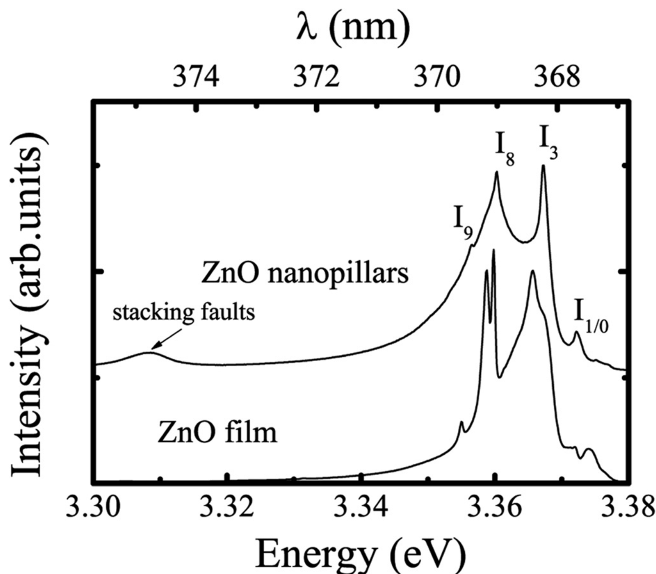

FIG. 5. Near-band-edge photoluminescence spectra at 8 K of the ZnO nanopillars (offset added for better visibility) and the overgrown ZnO film.

where the Burgers vectors are given by $\mathbf{b}_{\text{screw}} = [0001]$ and $\mathbf{b}_{\text{edge}} = 1/3[11\bar{2}0]$. We obtain densities of screw and edge type dislocations of $2.6 \times 10^8\,\text{cm}^{-2}$ and $2 \times 10^{10}\,\text{cm}^{-2}$, respectively.

For the examination of the optical properties, low-temperature PL experiments were carried out on both the pillars and the final layer. Figure 5 shows the excitonic region of the spectra. Different donor-bound excitons assigned mainly to Gallium (I_1, I_8) and Indium (I_9) dominate.[16] Interestingly, for the ZnO film also, the hydrogen-related line I_4 at 3.363 eV appears. Obviously, during our growth process, some atomic hydrogen is created from the isopropanol-oxygen reaction. The I_{8a} line is now the dominant one and becomes very sharp with a FWHM below 300 μeV. For the nanopillars, also a weaker broad peak centered at $\approx$3.31 eV is observed, which is introduced by basal plane stacking faults (BSFs).[17] During the initial growth phase of the ZnO pillars on the sapphire substrate, a higher abundance of imperfections like BSFs is expected. After overgrowth, this type of defect seems to be completely absent.

This concept of epitaxial overgrowth of aligned nanopillars to enforce a desired direction of the epitaxial layer opens a way to grow high quality epi-layers in controlled orientation. It might be especially useful for the growth of semi- or non-polar layers from hexagonal semiconductors like (Mg,Zn,Cd)O, (Al,Ga,In)N, etc., for which there is typically an increased tendency to polymorphism and inclusion of stacking faults when growing such non-high-symmetry planes. For some systems, there exist already recipes for the growth of tilted nanowires.[18] More generally, this method could be expanded by using ordered arrays of nanopillars generated on pre-patterned substrates, defined by nanosphere lithography[19] or laser interference lithography.[20] Then, it can—even on conventional substrate planes—replace the frequently used epitaxial lateral overgrowth (ELOG) technique[21] and can be used further to reduce the dislocation density of the final layer due to shorter distances of initial regions with perfect crystallinity. This method also has a high potential in the case of InGaN layers with higher In content needed for optical applications in the green/yellow regime to reduce the defect density and thus help to solve the "green gap" problem of low LED and laser efficiencies in this color range.

In summary, we reported a method for enforced *c*-axis oriented growth of ZnO films grown on *a*-plane sapphire mediated by nanopillars. The XRD ($\omega - 2\theta$)-scan shows the ZnO film to grow along the *c*-axis with only minor $(01\bar{1}1)$-oriented domains included. The FWHM of the (0002) rocking curve is below 400 arcsec, which indicates the suppressed screw dislocation density. Low-temperature PL shows extremely narrow donor-bound exciton emission with FWHM below 300 μeV. Any stacking fault related 3.31 eV luminescence disappeared after growth of the ZnO film over the primary ZnO nanopillars. This method opens an alternative way to reduce the dislocation density and to increase the quality and homogeneity of epilayers in similar heteroepitaxial systems.

We thank Wladimir Schoch for assistance in the XRD measurements. Y.X. is grateful for financial support from the China Scholarship Council (CSC) under No. 2007U31059.

[1]Ü. Özgür, Y. I. Alivov, C. Liu, A. Teke, M. A. Reshchikov, S. Doğan, V. Avrutin, S. J. Cho, and H. Morkoç, J. Appl. Phys. **98**, 041301 (2005).
[2]C. Klingshirn, J. Fallert, H. Zhou, J. Sartor, C. Thiele, F. Maier-Flaig, D. Schneider, and H. Kalt, Phys. Status Solidi B **247**(6), 1424 (2010).
[3]C. R. Gorla, N. W. Emanetoglu, S. Liang, W. E. Mayo, Y. Lu, M. Wraback, and H. Shen, J. Appl. Phys. **85**, 2595 (1999).
[4]S. Liang, H. Sheng, Y. Liu, Z. Huo, Y. Lu, and H. Shen, J. Cryst. Growth **225**, 110–113 (2001).
[5]X. W. Sun and H. S. Kwok, J. Appl. Phys. **86**, 408 (1999).
[6]E. M. Kaidashev, M. Lorenz, H. von Wenckstern, A. Rahm, H.-C. Semmelhack, K.-H. Han, G. Benndorf, C. Bundesmann, H. Hochmuth, and M. Grundmann, Appl. Phys. Lett. **82**, 3901 (2003).
[7]X. Du, Z. Mei, Z. Liu, Y. Guo, T. Zhang, Y. Hou, Z. Zhang, Q. Xue, and A. Y. Kuznetsov, Adv. Mater. **21**, 4625 (2009).
[8]A. Zeuner, H. Alves, D. M. Hoffmann, B. K. Meyer, M. Heuken, J. Blaesing, and A. Krost, Appl. Phys. Lett. **80**, 2078 (2002).
[9]M. M. C. Chou, L. W. Chang, D. R. Hang, C. L. Chen, D. S. Chang, and C. A. Li, Cryst. Growth Des. **9**, 2073 (2009).
[10]X. Wang, J. Song, and Z. L. Wang, J. Mater. Chem. **17**, 711 (2007).
[11]P. Fons, K. Iwata, A. Yamada, K. Matsubara, and S. Niki, K. Nakahara, T. Tanabe, and H. Takasu, Appl. Phys. Lett. **77**, 1801 (2000).
[12]A. Reiser, V. Raeesi, G. M. Prinz, M. Schirra, M. Feneberg, U. Roder, R. Sauer, and K. Thonke, Microelectron. J. **40**, 306 (2009).
[13]A. Reiser (private communication).
[14]H. von Wenckstern, H. Schmidt, C. Hanisch, M. Brandt, C. Czekalla, G. Benndorf, G. Biehne, A. Rahm, H. Hochmuth, M. Lorenz, and M. Grundmann, Phys. Status Solidi (RRL) **1**(4), 129 (2007).
[15]C. G. Dunn and E. F. Kogh, Acta Metall. **5**(10), 548 (1957).
[16]B. K. Meyer, H. Alves, D. M. Hofmann, W. Kriegseis, D. Forster, F. Bertram, J. Christen, A. Hoffmann, M. Strassburg, M. Dworzak, U. Haboeck, and A. V. Rodina, Phys. Status Solidi B **242**, 231 (2004).
[17]M. Schirra, R. Schneider, A. Reiser, G. M. Prinz, M. Feneberg, J. Biskupek, U. Kaiser, C. E. Krill, K. Thonke, and R. Sauer, Phys. Rev. B **77**, 125215 (2008).
[18]J. Zuniga-Perez, A. Rahm, C. Czekalla, J. Lenzner, M. Lorenz, and M. Grundmann, Nanotechnology **18**, 195303 (2007).
[19]D. F. Liu, Y. J. Xiang, X. C. Wu, Z. X. Zhang, L. F. Liu, L. Song, X. W. Zhao, S. D. Luo, W. J. Ma, J. Shen, W. Y. Zhou, G. Wang, C. Y. Wang, and S. S. Xie, Nano Lett. **6**, 2375 (2006).
[20]Y. G. Wei, W. Z. Wu, R. Guo, D. J. Yuan, S. M. Das, and Z. L. Wang, Nano Lett. **10**, 3414 (2010).
[21]O.-H. Nam, M. D. Bremser, T. S. Zheleva, and R. F. Davis, Appl. Phys. Lett. **71**, 2638 (1997).